JOURNAL OF Materials CHEMISTRY

Synthesis and characterisation of a linear $[Cu(pyr)_2]^{2+}$ complex in siliceous ferrierite

Martin P. Attfield,[a] Scott J. Weigel,[b] Francis Taulelle[c] and Anthony K. Cheetham*[a]

[a]*Materials Department, University of California, Santa Barbara, CA 93106, USA. E-mail: cheetham@mrl.ucsb.edu*
[b]*Chemistry Department, University of California, Santa Barbara, CA 93106, USA*
[c]*RMN et Chimie du Solide, UMR 7510 ULP-Bruker-CNRS, Universite Louis Pasteur, 4 rue Blaise Pascal, 67070 Strasbourg Cedex, France*

Received 14th April 2000, Accepted 27th June 2000
Published on the Web 7th August 2000

The linear $[Cu(pyr)_2]^{2+}$ complex has been synthesized *in situ* within the internal pore architecture of siliceous ferrierite. The structure of the product was determined by single crystal X-ray diffraction [formula $Cu_{0.964}F_{1.2}(Si_{36}O_{72})\cdot 4C_5H_5N$, space group *Pmnn*, $a=18.775(1)$, $b=14.086(1)$, $c=7.4296(6)$ Å, $V=1964.9(4)$ Å^3, $Z=1$, $R(F)=3.88$, $Rw(F)=4.31\%$]. The complex consists of a Cu^{2+} cation located at the center of the 8-ring window bound to one pyridine molecule residing in the cage that forms part of the 8-ring channel and another pyridine molecule in the main 10-ring channel. Evidence for the presence of this complex is also provided by EPR. The charge of the complex is balanced by F^- anions, which were found in the crystal structure to be present in SiO_4F^- units, and SiO_3O^- defect sites in the zeolite framework. The presence of both the SiO_4F^- units and the SiO_3O^- defect sites was confirmed by NMR spectroscopy.

1 Introduction

The incorporation of metal complexes and organometallic compounds into the cages and channels of zeolites is an area of considerable interest because of the possibility of combining the unique properties of the host with that of the encapsulated species.[1] Particular attention has focused on the possibility of forming organised micro-assemblies of metal or semiconductor particles in the zeolite from the encapsulated precursors,[2,3] and the catalytic behavior of these hybrid materials, as they allow the combination of the specific activity of the metal complex and the shape selectivity of the microporous material into one catalyst.[1,4] Typically, the formation of metal complexes in the zeolite has been achieved by post-synthesis procedures,[1] but it is also possible to incorporate the metal complex by adding the complex directly into the synthesis mixture.[5–8] This process can lend itself to the formation of new structures, for example, the 14-membered ring zeolite $[(Cp^*)_2Co^+]$-UTD-1,[9] the metallic complex acting as a structure directing agent in the synthesis of the zeolite.

Work on the hydrothermal synthesis of ferrierite[10–12] has shown that large single crystals may be synthesized using a HF–pyridine solvent system in the presence of propylamine. Such a system provides the opportunity to prepare metal pyridine complexes *in situ* within the pore structure of ferrierite. As this type of synthesis tends to form large single crystals, diffraction techniques may be used to study the structure and location of the metal complex within the zeolite framework. Copper was selected for incorporation, since copper(II)–pyridine derivatives encapsulated in faujasite have been shown to be active catalysts in the oxidative coupling of 2,6-dimethylphenol[13] and copper has been shown to be the active site in Cu-exchanged zeolitic deNO_x catalysts.[14] The use of the ferrierite framework may also impose shape selectivity upon reactions catalyzed within its pores, as has been exemplified by the isomerization of n-butenes to isobutene.[15]

The structure of ferrierite was first determined by Vaughan[16] and Kerr,[17] although there is still discussion as to the correct symmetry of the material.[18–20] The framework of ferrierite is based on 5-ring building units that are stacked parallel to the [001] direction. The connection of these rings forms an oval 10-ring channel (pore dimensions 4.2 by 5.4 Å) running along the [001] direction, which is intersected by an 8-ring channel (pore dimensions 3.5 by 4.8 Å) that runs along the [010] direction. The two channels are shown in Fig. 1a and b, respectively. The 8-ring channel may also be considered as consisting of cages, bounded by 6-rings and 8-rings, that connect the 10-ring channels. As far as the authors are aware, there are no known structures of metallic complexes in ferrierite. The locations of alkali, alkaline metal and Cu^{2+} cations have been reported,[21–23] and the structure of deuterated ferrierite has recently been determined.[24]

In this paper we report the synthesis and characterization of a linear $[Cu(pyr)_2]^{2+}$ complex formed *in situ* within siliceous ferrierite.

2 Experimental

2.1 Synthesis

A batch of single crystals of siliceous ferrierite was synthesised according to the method of Kuperman *et al.*,[10] but with $Cu(NO_3)_2\cdot 2.5H_2O$ added to the starting solution. The reactants used were pyridine (Fisher, pyr), propylamine (Aldrich, $PrNH_2$), HF–pyridine (Aldrich, 70 wt% HF), Cab-O-Sil (Acros, M-5 grade) and deionised water. The oxide molar ratio for this reaction was: 1.5 SiO_2 : 2 HF–pyr : 0.375 CuO : 8 H_2O : 4 $PrNH_2$: 16 pyr.

Appropriate amounts of propylamine, pyridine, HF–pyridine, and half of the water were added to a 23 ml Teflon liner. Cab-O-Sil was then added slowly to the amine solution and stirred for 1 h to dissolve the silica. The $Cu(NO_3)_2$ was dissolved in the remaining water before being added to the clear silicate solution. The resulting clear blue solution was stirred for an additional 30 min. The reaction mixture was then sealed in a Parr digestion bomb and heated under hydrothermal conditions at 170 °C for 6 days. The product was filtered, washed with water, rinsed with acetone and dried under ambient conditions. The product consisted of single crystals and amorphous material, which were separated by sonication.

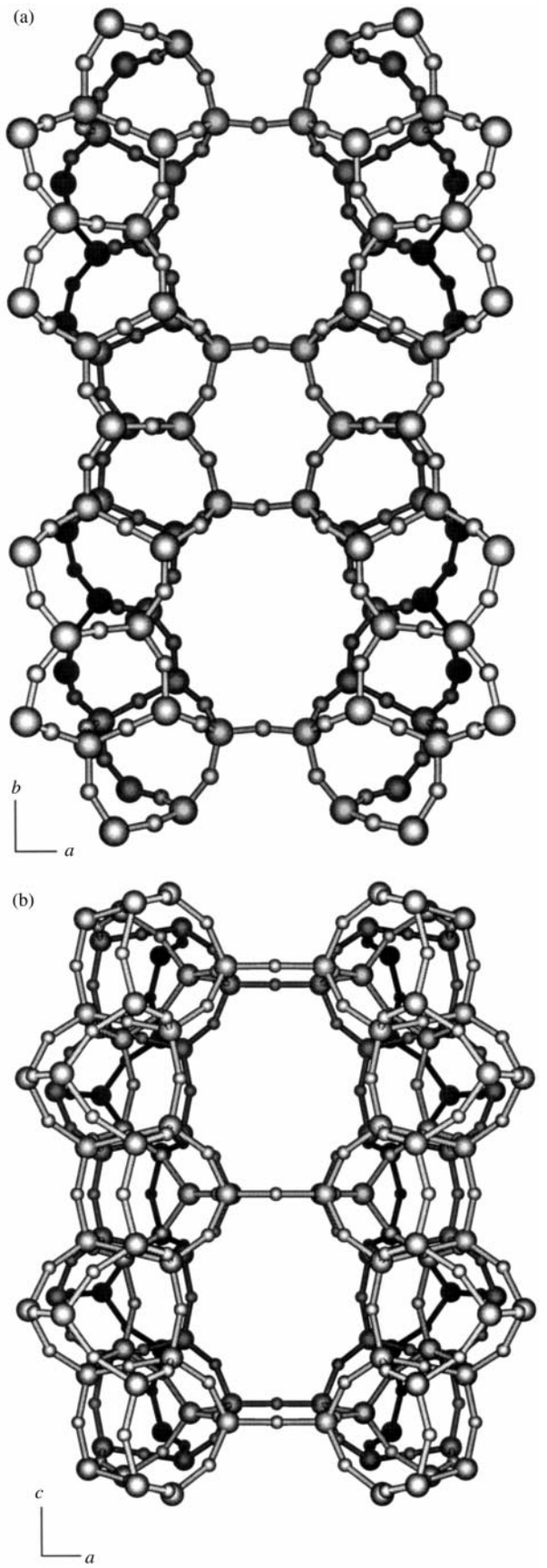

Fig. 1 The structure of ferrierite viewed (a) along the [001] direction, showing the 10-ring channel, and (b) along the [010] direction, showing the 8-ring channel.

The large single crystals obtained were pale blue in colour. Microprobe analysis of the single crystals gave a composition of $Cu_{0.94}F_{0.86}(SiO_2)_{36}$; the microprobe analysis was performed on a Cameca SX50 electron probe microanalyzer, using copper metal, albite ($Na_{0.25}Al_{0.25}Si_{0.75}O_2$), and durango [$Ca_5(PO_4)_3F$] as standards.

2.2 Crystal structure determination

A single crystal suitable for structure determination was mounted on a CAD4-MACH X-ray diffractometer, equipped with a Rigaku rotating anode source, and room temperature diffraction data were collected.

The systematic absences were consistent with those of the orthorhombic space group *Pmnn* (no. 58). The siliceous ferrierite framework structure reported in this space group[20] was used as the starting model for the structure solution. The extra-framework copper, nitrogen, carbon, fluorine and hydrogen atoms were all located from difference Fourier syntheses. The final cycle of least-squares refinement, against *F*, included anisotropic refinement for all the non-hydrogen atoms and free refinement of the occupancies of the extra-framework copper and fluorine sites. The occupancies of the constituent atoms of the pyridine molecules were not refined. The isotropic temperature factors of the hydrogen atoms were held at reasonable values and one of the hydrogen atoms was held in 'riding' mode during refinement. Crystallographic details for the structure are given in Table 1. Final fractional atomic coordinates, equalised temperature factors and occupancies are provided in Table 2. Selected bond distances and angles are given in Table 3. All least-squares, Fourier and subsidiary calculations were performed using CRYSTALS.[25]

CCDC 1145/229. See http://www.rsc.org/suppdata/jm/b0/b003005h/ for crystallographic data (in MS WORD .doc format).

2.3 Spectroscopic analysis

The EPR spectrum was collected at 10 K on a Bruker ESP-300 spectrometer operating in the X-band at a frequency of 9.460 GHz. The sample was contained in a 4 mm o.d. sealed quartz tube. Before sealing, the tube was evacuated at *ca.* 10^{-6} Torr for 15 min. The calibration standard used was DPPH, which gave a *g*-value of 2.008. The observed EPR spectrum was simulated using the program POWDER.[26]

The ^{19}F and ^{29}Si MAS NMR spectra of the sample were collected at room temperature on Chemagnetics CMX500 and Bruker DSX500 spectrometers, respectively. The chemical shifts were referenced relative to $CFCl_3$ and TMS, both at 0 ppm, for ^{19}F and ^{29}Si NMR, respectively.

Table 1 Crystallographic data for $[Cu(pyr)_2]^{2+}$-containing siliceous ferrierite

Formula	$Cu_{0.964}F_{1.2}(Si_{36}O_{72})\cdot 4C_5H_5N$
Molecular weight	2563.52
Crystal system	Orthorhombic
a/Å	18.775(1)
b/Å	14.086(1)
c/Å	7.4296(6)
V/Å^3	1964.9(4)
Temperature/K	298
Space group	*Pmnn* (no. 58)
Z	1
μ(Cu-Kα)/cm^{-1}	70.91
No. of reflections	4780
No. of independent reflections	1993
R_{int} (%)	3.16
$R(F)$ [$I>3\sigma(I)$] (%)	3.88
$R_w(F)$ [$I>3\sigma(I)$] (%)	4.31

Table 2 Final atomic coordinates, equalised temperature factors and occupancy factors for $[Cu(pyr)_2]^{2+}$-containing siliceous ferrierite

Atom	*x*	*y*	*z*	*U*(eq)/Å^2	Occupancy
Si(1)	0.15393(7)	0.0000	0.0000	0.0127	1.000
Si(2)	0.27373(5)	−0.00196(9)	0.2931(1)	0.0137	1.000
Si(3)	0.08396(5)	−0.20054(7)	−0.0095(1)	0.0145	1.000
Si(4)	0.17249(5)	−0.30161(7)	0.2837(1)	0.0140	1.000
Si(5)	0.17921(5)	−0.29441(8)	−0.3055(1)	0.0149	1.000
O(1)	0.2498(2)	0.0000	0.5000	0.0221	1.000
O(2)	0.2026(2)	0.0035(3)	0.1759(4)	0.0294	1.000
O(3)	0.1038(2)	−0.0909(2)	0.0074(5)	0.0278	1.000
O(4)	0.1540(2)	−0.2803(2)	0.4896(4)	0.0215	1.000
O(5)	0.0000	−0.2117(3)	−0.0243(6)	0.0250	1.000
O(6)	0.2463(2)	−0.2555(3)	0.2298(6)	0.0369	1.000
O(7)	0.1191(2)	−0.2448(3)	−0.1862(4)	0.0287	1.000
O(8)	0.1100(2)	−0.2568(2)	0.1660(4)	0.0256	1.000
O(9)	0.3247(1)	0.0865(2)	0.2507(4)	0.0255	1.000
O(10)	0.3178(2)	−0.0963(2)	0.2508(5)	0.0282	1.000
Cu(1)	0.5000	0.7474(4)	0.0146(9)	0.0639	0.241(6)
F(1)	0.259(1)	−0.337(1)	−0.460(2)	0.0333	0.15(1)
N(1)	0.5000	0.6000(8)	−0.001(1)	0.0801	1.000
C(11)	0.5624(4)	0.5477(5)	0.001(1)	0.0636	1.000
N(2)	0.5000	0.903(2)	−0.009(8)	0.1176	1.000
C(21)	0.5000	0.957(4)	−0.164(6)	0.1382	1.000
C(22)	0.5000	0.954(3)	0.151(6)	0.1251	1.000
H(11)	0.605(4)	0.581(4)	−0.027(8)	0.0500	1.000
H(21)	0.5000	0.925(7)	−0.32(1)	0.0500	1.000
H(22)	0.5000	0.914(3)	0.262(6)	0.0500	1.000

3 Results and discussion

The crystal structure of the copper–pyridine-containing siliceous ferrierite is shown in Fig. 2. The chemical composition calculated from the structure determination is $Cu_{0.96}F_{1.20}$-$(SiO_2)_{36}$·4(C_5H_5N), with a Cu/Si ratio of 0.027 and a Cu/F ratio of 0.80. Microprobe analysis on a single crystal gave a Cu/Si = 0.026 and Cu/F = 1.08, in reasonable agreement with the values obtained from the refinement. The agreement of the Cu/F ratios is less exact than for the Cu/Si ratio due to the limitations of microprobe analysis for detecting small amounts of fluorine. The Si–O bond lengths are all extremely close to the ideal value of 1.60 Å, indicating that the zeolite framework has been accurately determined. Refinement of the structure in the space group *Pmnn* prevents the imposition of chemically unfavorable 180° Si–O–Si bond angles on the framework structure, which is reflected in the closing of the Si(4)–O(6)–Si(5) angle from 180 to 174.7°.

The linear $[Cu(pyr)_2]^{2+}$ complex formed consists of a Cu^{2+} cation located at the center of the 8-ring window bound to one pyridine molecule residing in the cage that forms part of the 8-ring channel and another pyridine molecule in the main 10-ring channel. The planes of the two pyridine molecules bound to each Cu^{2+} cation are arranged orthogonally with respect to each other, as is shown in Fig. 3. The Cu^{2+} cations are 2.934(4) Å from the closest framework oxygen atoms (O_z), O(4), which suggests any direct interaction with them is weak; thus it is the interaction with the nitrogen atoms of the two pyridine molecules in the formation of the complex that allows incorporation of the Cu^{2+} cations inside the siliceous structure. This is seen in the shorter Cu–N bond lengths of 2.08(1) and 2.20(2) Å, which are in agreement with values for Cu^{2+} cations found in other Cu(II)–pyridine coordination complexes, such as polymeric $[Cu(CN)(pyr)_2]$[27] (Cu–N bond lengths range from 1.953 to 2.201 Å) and $Cu(ClO_4)_2(pyr)_4$[28] (Cu–N bond lengths range from 2.006 to 2.042 Å).

The same locations for both of the pyridine molecules in this study have been reported in other studies of uncalcined siliceous ferrierite.[11,12] Of the two crystallographically different pyridine molecules, the one located in the cage of the 8-ring channel is more tightly bound within the zeolite, as is indicated by the smaller thermal parameters of its atoms. Both pyridine sites are fully occupied, so the number of pyridine molecules required to bind to the Cu^{2+} cations is in 2-fold excess. This indicates that the pyridine molecules are held in place by their

Table 3 Selected bond lengths, non-bonding distances (Å) and bond angles (°) for $[Cu(pyr)_2]^{2+}$-containing siliceous ferrierite

Average Si(1)–O bond length 1.592(3)			
Average Si(2)–O bond length 1.600(3)			
Average Si(3)–O bond length 1.595(3)			
Average Si(4)–O bond length 1.593(3)			
Si(5)–O(4)	1.606(3)	Si(5)–O(6)	1.587(4)
Si(5)–O(7)	1.597(3)	Si(5)–O(10)	1.597(3)
Si(5)–F(1)	1.99(2)		
Weighted average Si–O bond length 1.596			
Cu(1)–N(1)	2.08(1)	Cu(1)–N(2)	2.20(2)
Cu(1)–O(4) × 2	2.934(4)		
F(1)···O(4)	2.17(2)	F(1)···O(6)	1.92(2)
F(1)···O(10)	2.33(2)		
Average O–Si(1)–O bond angle 109.5(2)			
Average O–Si(2)–O bond angle 109.5(2)			
Average O–Si(3)–O bond angle 109.5(2)			
Average O–Si(4)–O bond angle 109.1(2)			
O(4)–Si(5)–O(6)	111.2(2)	O(4)–Si(5)–O(7)	105.3(2)
O(6)–Si(5)–O(7)	109.7(2)	O(4)–Si(5)–O(10)	112.2(2)
O(6)–Si(5)–O(10)	110.6(2)	O(7)–Si(5)–O(10)	107.6(2)
O(4)–Si(5)–F(1)	73.3(5)	O(6)–Si(5)–F(1)	64.0(6)
O(7)–Si(5)–F(1)	171.6(6)	O(10)–Si(5)–F(1)	80.4(5)
N(1)–Cu(1)–N(2)	172.3(16)	O(4)–Cu(1)–O(4)	160.4(2)
N(1)–Cu(1)–O(4) × 2	98.9(1)	N(2)–Cu(1)–O(4) × 2	80.6(1)

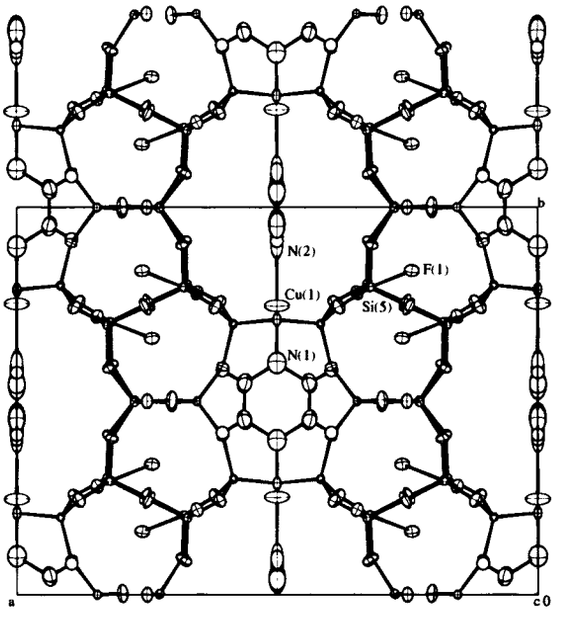

Fig. 2 The crystal structure of $[Cu(pyr)_2]^{2+}$-containing siliceous ferrierite viewed along the [001] direction. Thermal ellipsoids are drawn at 30% probability.

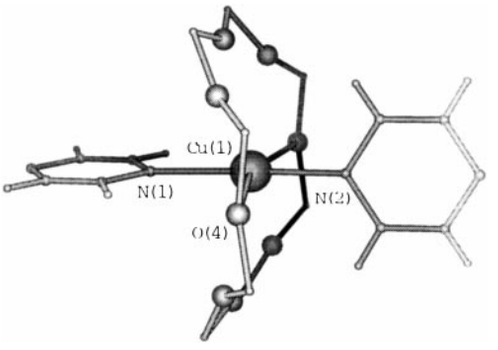

Fig. 3 The structure of the linear $[Cu(pyr)_2]^{2+}$ complex in the 8-ring of ferrierite. Only the shortest Cu–O_z bonds are included.

van der Waals interactions with the O_z atoms when the Cu^{2+} cations are not present.

The charge of the Cu^{2+} cations is partly compensated for by the negative charge of the fluoride anions. These are located between 5-rings within a [5^4] cage, as shown in Fig. 4. They interact with the Si(5) atom at a distance of 1.99(2) Å and have an apparent close contact of 1.92(2) Å to O(6). The O(6) atoms close to F(1) are presumably displaced in the tetrahedra where the F^- anions are present, but this is not observed in the structure as the occupancy of the F(1) site is only 15%. The location of the F^- anions is unusual, in that fluorine bound to silicon in a zeolite has only been found by diffraction techniques in siliceous nonasil[5] and SSZ-23,[29] and has never been observed in a small cage that does not contain a 4-membered ring. Typically, F^- anions have been found to occupy fairly central positions in small cages at distances greater than 2.20 Å from the nearest silicon atom.[30–32] The presence of five-coordinate silicon was reported in the nonasil structure,[5] where the Si–F bond length was 1.836(6) Å and the oxygen environment of the Si atom is distorted from the usual tetrahedral arrangement to that of a trigonal bipyramid, the F^- anion occupying the fifth vertex. In our ferrierite structure, the oxygen coordination of the Si(5) atom is still apparently tetrahedral, presumably because the low occupancy of F^- sites means that few $Si(5)O_4$ tetrahedra are distorted and the F^- anion is further from the Si(5) atom [1.99(2) Å] which will result in a lower distorting influence. A similar situation was observed in the structure of as-synthesised SSZ-23,[29] where the occupancy of the F^- sites was too low for the distortion of the associated SiO_4 tetrahedra to be detected in the structure and the Si–F bond lengths are in the range 1.94 to 1.96 Å. The F^- anions are found to be a long way away [5.03(2) Å] from the Cu^{2+} cations. A similar phenomenon has been observed in the structures of some as-prepared clathrasils. A large separation of the F^- anion and the positive charge center have been reported in [$Co^+(\eta^5\text{-}C_5H_5)_2F^-$]-nonasil,[5] where the shortest Co–F bond distance is 6.43 Å, and in octadecasil.[30] The large distance between the charges must be due to the dielectric shielding properties of the silica framework.

The observed and simulated EPR spectra of the sample are shown in Fig. 5 and contain a broad signal indicative of one Cu^{2+} species with EPR parameters of $g_{\|}=2.281$, $A_{\|}=189\times10^{-4}\,cm^{-1}$, $g_{\perp(yy)}=2.058$ and $g_{\perp(xx)}=2.055$. These parameters are similar to those obtained for the $[Cu(pyr)_2]^{2+}$ complex formed when Cu-ZSM-5 was exposed to pyridine vapour ($g_{\|}=2.25$, $A_{\|}=187\times10^{-4}\,cm^{-1}$ and $g_{\perp}=2.05$).[33] The EPR data support the findings of the X-ray structure determination, that such a complex is present in this sample of ferrierite.

The ^{19}F MAS NMR spectrum of the sample is shown in Fig. 6 and shows a single peak with many spinning sidebands.

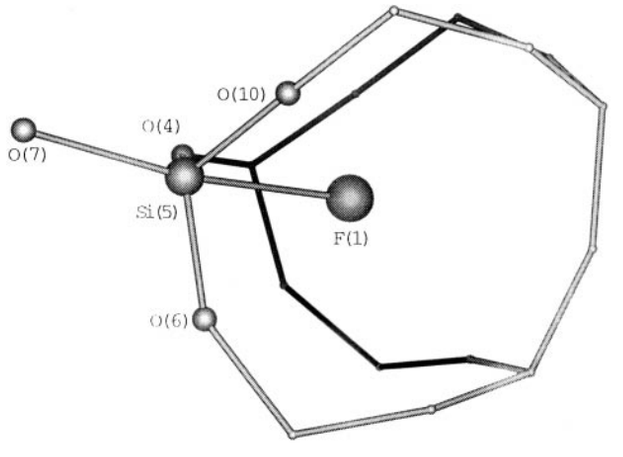

Fig. 4 Illustration of the 5-coordinate Si(5) atom in the ferrierite framework. Only the atoms directly bound to Si(5) are shown.

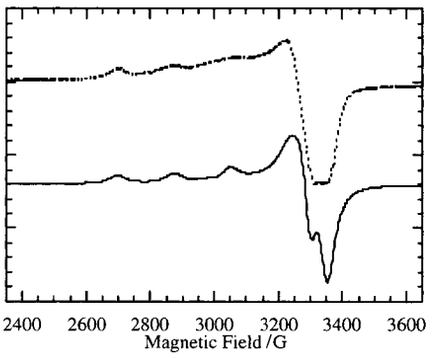

Fig. 5 Experimental (dashed) and simulated (solid) EPR spectra of $[Cu(pyr)_2]^{2+}$-containing siliceous ferrierite.

The isotropic resonance was determined by collecting spectra at different spinning frequencies. The appearance of one signal indicates there is only one type of fluorine environment in the structure, as suggested by the crystallographic findings. The asymmetry of the spectrum indicates that the fluorine environment is not symmetrical, which is in agreement with the location of the fluorine in the crystal structure, as shown in Fig. 4. The chemical shift of the signal (−59.5 ppm) lies in the range previously found for fluorine in other siliceous zeolites (−56.4 to −78.1 ppm).[34,35]

The ^{29}Si MAS NMR spectrum of the sample is shown in Fig. 7 and is dominated by the Q^4 Si resonances of the ferrierite framework between −107.7 and −116.9 ppm, as seen for other siliceous ferrierite samples.[11] In addition to the Q^4 resonances, smaller peaks at approximately −100.7 ppm (5.6% relative intensity) and −147.6 ppm (3.6% relative intensity) are visible in the spectrum and are assigned to a Q^3 Si resonance and a pentacoordinated Si atom in a SiO_4F^- site, respectively. The chemical shift for the pentacoordinated silicon is in the region expected for SiO_4F^- units in which the F^- anions are localised to one particular silicon site, as is seen in the room temperature $^{29}Si\{^1H\}$ CPMAS NMR spectra for [$Co^+(\eta^5\text{-}C_5H_5)_2F^-$]-nonasil[36] and as-synthesised ITE, BEA and MTW,[35] where the silicons of the SiO_4F^- units resonate in the range −140 to −150 ppm.[35] The F/Si ratio predicted from the structure determination is 0.033 which is in excellent agreement with the fraction of pentacoordinated silicon (0.036) determined from the NMR spectrum, implying all the fluorine in the structure is contained within the SiO_4F^- units. The Q^3 silicon indicates the presence of ≡Si–O^- or ≡Si–OH groups in the ferrierite framework. Such groups are found at defect sites in the zeolite framework and are formed from cleavage of a Si–O–Si bond.

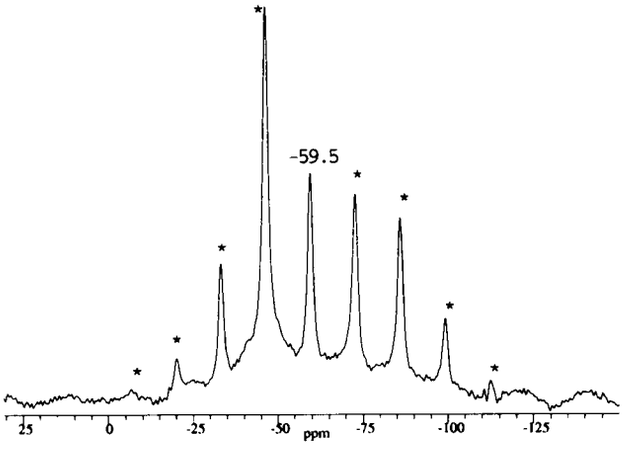

Fig. 6 The ^{19}F MAS NMR spectrum of $[Cu(pyr)_2]^{2+}$-containing siliceous ferrierite. The spinning sidebands are marked with asterisks (*).

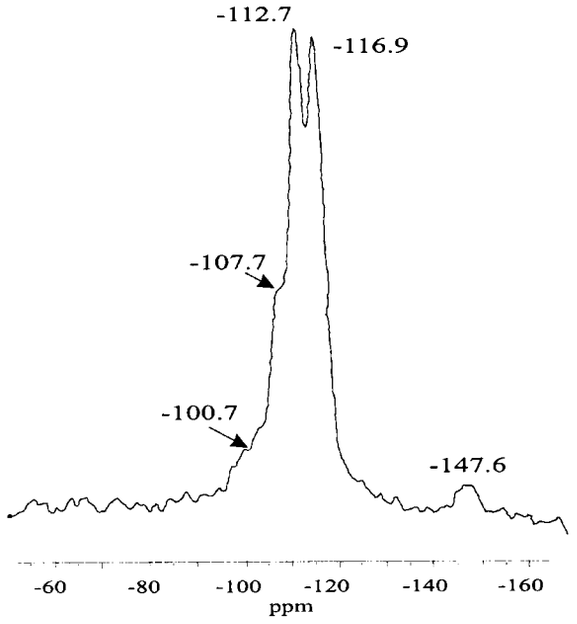

Fig. 7 The ^{29}Si MAS NMR spectrum of $[Cu(pyr)_2]^{2+}$-containing siliceous ferrierite.

The $\equiv Si–O^-$ groups present at the framework defect sites help to balance the positive charge of the Cu^{2+} cations. The extra negative charge introduced into the system by the $\equiv Si–O^-$ groups is necessary because the total negative charge of F^- anions in the formula unit is not enough to balance the total positive charge of the Cu^{2+} cations in the same unit. Inclusion of the framework defect sites in the molecular formula would give a charge balanced formula of $Cu_{0.964}F_{1.2}Si_{36}O_{72}(OH)_{0.73}]\cdot 4C_5H_5N$. However, we report the formula $Cu_{0.964}F_{1.2}(Si_{36}O_{72})\cdot 4C_5H_5N$, derived from the crystallographic results, as it is difficult to quantify the number of framework defects and there might be more defect sites than is necessary to compensate for the charge of the Cu^{2+} cations not balanced by the F^- anions.

4 Conclusions

A linear $[Cu(pyr)_2]^{2+}$ complex has been formed *in situ* inside the pore system of siliceous ferrierite and its structure determined by X-ray diffraction and spectroscopic techniques. The coordination of the metal complex is controlled by the architecture of the zeolite, as illustrated by the formation of the binary pyridine complex and not the more common tetrahedral complex. Only the binary complex can fit easily within the channels of ferrierite, whereas the larger cavity of faujasite can contain the bulkier tetrahedral complex. This exemplifies the potential use of zeolites to isolate specific metal complexes. The formation of the $[Cu(pyr)_2]^{2+}$ complex in the manner we have described highlights the possibility of forming other similar complexes by the inclusion of molecules like pyrazine into the synthesis mixture. Such a method would provide the opportunity of forming chains of $[Cu(pyrazine)_2]$ throughout the structure. These single chains could well exhibit interesting optical and electronic properties.

Acknowledgements

The work was funded by the MRL program of the National Science Foundation award DMR 9123048 and Los Alamos National Laboratory. We would also like to thank Dr Lucy Bull for her help with the collection of the NMR data.

References

1 G. A. Ozin and C. Gil, *Chem. Rev.*, 1989, **89**, 1749.
2 C. L. Bowes and G. A. Ozin, *J. Mater. Chem.*, 1998, **8**, 1281.
3 G. D. Stucky and J. E. MacDougall, *Science*, 1990, **247**, 669.
4 W. Kahlen, H. H. Wagner and W. E. Holderich, *Catal. Lett.*, 1998, **54**, 85.
5 G. van de Goor, C. Freyhardt and P. Behrens, *Z. Anorg. Allg. Chem.*, 1995, **621**, 311.
6 K. J. Balkus and S. Shepelev, *Microporous Mater.*, 1993, **1**, 383.
7 K. Morgan, G. Gainsford and N. Milestone, *J. Chem. Soc., Chem. Commun.*, 1995, 425.
8 D. J. Williams, J. S. Kruger, A. F. McLeroy, A. P. Wilkinson and J. C. Hanson, *Chem. Mater.*, 1999, **11**, 2241.
9 C. C. Freyhardt, M. Tsapatsis, R. F. Lobo, K. J. Balkus and M. E. Davis, *Nature*, 1996, **381**, 295.
10 A. Kuperman, S. Nadimi, S. Oliver, G. A. Ozin, J. M. Garces and M. M. Olken, *Nature*, 1993, **365**, 239.
11 S. J. Weigel, J. C. Gabriel, E. Guttierez Puebla, A. Monge Bravo, N. J. Henson, L. M. Bull and A. K. Cheetham, *J. Am. Chem. Soc.*, 1996, **118**, 2427.
12 J. E. Lewis, C. C. Freyhardt and M. E. Davis, *J. Phys. Chem.*, 1996, **100**, 5039.
13 Y. Ukisu, A. Kazusaka and M. Nomura, *J. Mol. Catal.*, 1991, **70**, 165.
14 M. Shelef, *Chem. Rev.*, 1995, **95**, 209.
15 H. H. Mooiweer, K. P. de Jong, B. Kraushaar-Czarnetzki, W. H. J. Stork and B. C. H. Krutzen, *Stud. Surf. Sci. Catal.*, 1994, **84**, 2327.
16 P. A. Vaughan, *Acta Crystallogr.*, 1966, **21**, 983.
17 I. S. Kerr, *Nature*, 1966, **210**, 294.
18 R. Gramlich-Meier, V. Gramlich and W. M. Meier, *Am. Mineral.*, 1985, **70**, 619.
19 A. Alberti and C. Sabelli, *Z. Kristallogr.*, 1987, **178**, 249.
20 R. E. Morris, S. J. Weigel, N. J. Henson, L. M. Bull, M. T. Janicke, B. F. Chmelka and A. K. Cheetham, *J. Am. Chem. Soc.*, 1994, **116**, 11849.
21 W. J. Mortier, *Compilation of Extra-framework Sites in Zeolites*, Butterworth, Guildford, 1982.
22 I. J. Pickering, P. J. Maddox, J. M. Thomas and A. K. Cheetham, *J. Catal.*, 1989, **119**, 261.
23 M. P. Attfield, S. J. Weigel and A. K. Cheetham, *J. Catal.*, 1997, **172**, 274.
24 A. Martucci, A. Alberti, G. Cruciani, P. Radaelli, P. Ciambelli and M. Rupacciulo, *Microporous Mesoporous Mater.*, 1999, **30**, 95.
25 D. J. Watkin, J. R. Carruthers and P. W. Betteridge, *CRYSTALS User Guide*, Chemical Crystallography Laboratory, Oxford, 1990.
26 C. Daul, C. W. Schlapfer, J. Ammeter and E. Gamp, *Comput. Phys. Commun.*, 1981, **21**, 385.
27 M. M. Olmstead, *Acta. Crystallogr., Sect. C*, 1993, **49**, 370.
28 M. Labarelle, R. Louis and B. Metz, *Acta Crystallogr., Sect. C*, 1994, **50**, 536.
29 M. A. Camblor, M.-J. Diaz-Cabanas, J. Perez-Pariente, S. J. Teat, W. Clegg, I. J. Shannon, P. Lightfoot, P. A. Wright and R. E. Morris, *Angew. Chem., Int. Ed.*, 1998, **37**, 2122.
30 P. Caullet, J. L. Guth, J. Hazm, J. M. Lamblin and H. Gies, *Eur. J. Solid State Inorg. Chem.*, 1991, **28**, 345.
31 P. A. Barrett, M. A. Camblor, A. Corma, R. H. Jones and L. A. Villaescusa, *J. Phys. Chem. B*, 1998, **102**, 4147.
32 G. D. Price, J. J. Pluth, J. V. Smith, J. M. Bennet and L. R. Patton, *J. Am. Chem. Soc.*, 1982, **104**, 5971.
33 Y. Sendoda and Y. Ono, *Zeolites*, 1986, **6**, 209.
34 H. Koller, A. Wolker, S. Valencia, L. A. Villaescusa, M. J. Diaz-Cabanas and M. A. Camblor, in *Proceedings of the 12th International Zeolite Conference*, ed. M. M. J. Treacy, B. K. Marcus, M. E. Bisher and J. B. Higgins, Materials Research Society, Warrendale, USA, 1998, vol. 4, p. 2951.
35 H. Koller, A. Wolker, L. A. Villaescusa, M. J. Diaz-Cabanas, S. Valencia and M. A. Camblor, *J. Am. Chem. Soc.*, 1999, **121**, 3368.
36 H. Koller, A. Wolker, H. Eckert, C. Panz and P. Behrens, *Angew. Chem., Int. Ed. Engl.*, 1997, **36**, 2823.